Why do Giant Earthquakes Occur at Lunar Phases Specific to Each Subduction Zone?

Yoshiaki Fujii[a]*, Yuki Ozaki[a], Daisuke Fukuda[a] and Jun-ichi Kodama[a]

[a]*Hokkaido University, Sapporo, Japan*
*fujii6299@frontier.hokudai.ac.jp (*corresponding author's E-mail)*

Abstract

To clearly show the dangerous lunar phases during which giant earthquakes tend to occur at each subduction zone and to clarify the mechanisms of giant earthquake occurrences during neap tides at some subduction zones, the folded and double-folded lunar phase is introduced. The dangerous lunar phases for each subduction zone, represented as delays from spring tides, are 1 to 4 days for Peru, 3 to 5 days for Indonesia, 5 to 7 days for Tonga, 3 to 8 days for Japan, 8 to 11 days for Kuril, -3 to 0 days for Chile, -2 to 0 days for New Guinea, and -2 to 0 days for Alaska. Paying sufficient attention to foreshocks and various precursors such as GPS (Global Positioning System) anomalies during the dangerous lunar phase for each subduction zone will be a very useful way to reduce damage from giant earthquakes. The influence of the solid tidal stress on reverse faulting was investigated based on the strike of subduction zones, and prohibition of giant earthquakes caused by strength increase due to the rapid variation in tidal stress during spring tides at NS subduction zones was proposed as one reason why giant earthquakes occur not only at spring tides but also at neap tides at some subduction zones.

Keywords: Giant earthquakes, Lunar phase, Subduction zone, Stress rate, Strike

1. Introduction

Solid tidal stress is caused by the difference in the attraction vectors from the Moon and the Sun from point to point on and in the Earth, and it varies with the relative positions of the Sun, Earth, and Moon at periods of approximately 12 h (high and ebb tides) by rotation of the Earth, approximately one half month (spring and neap tides) by revolution of the Moon, approximately one half year by revolution of the Earth with its inclined axis of rotation, and at longer periods because the orbits of the Earth and Moon are not perfect circles and are not in the same plane (Gutzwiller, 1998). Solid tidal stress decreases confinement and increases shear stress at a subduction zone just beneath the Sun or the Moon (Fig. 1). The amplitude of the solid tidal stress is highest at spring tide, around the new moon (day 0 of the lunar cycle) or full moon (day 14.8 of the lunar cycle) phase, in which the Sun, Earth, and Moon are aligned and the solid tidal stresses by the Sun and the Moon interact with each other to produce an increased solid tidal stress (Fig. 2). The solid tidal stress is the lowest at neap tide, around the half moon (days 7.4 and 22.1 of the lunar cycle) phases, in which the Sun, Earth, and Moon form a right angle and the solid tidal stresses by the Sun and the Moon interact with each other to produce a decreased solid tidal stress (Fig. 2).

The phases of tidal movement and the solid tidal stress are different due to water mass responsiveness, and the difference can be as large as 12 h. Tidal movement causes a much larger stress by resonance of seawater than does the solid tidal stress, and the total of these is called the tidal stress. However, the amplitude of the tidal stress is large at spring tide and small at neap tide as is the solid tidal stress. Therefore, it is expected that spring tides could induce giant earthquakes.

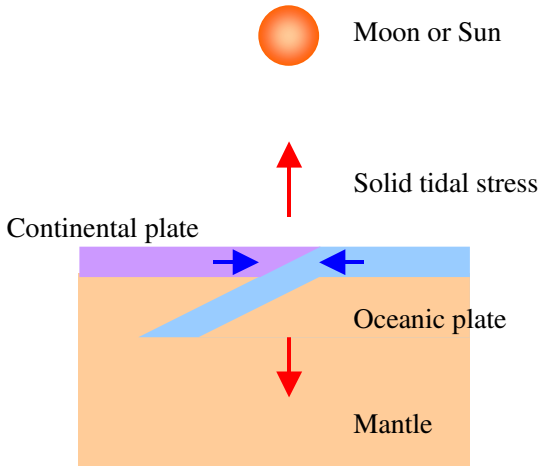

Figure 1. Schematic figure showing how solid tidal stress decreases confinement and increases shear stress beneath the Moon or Sun.

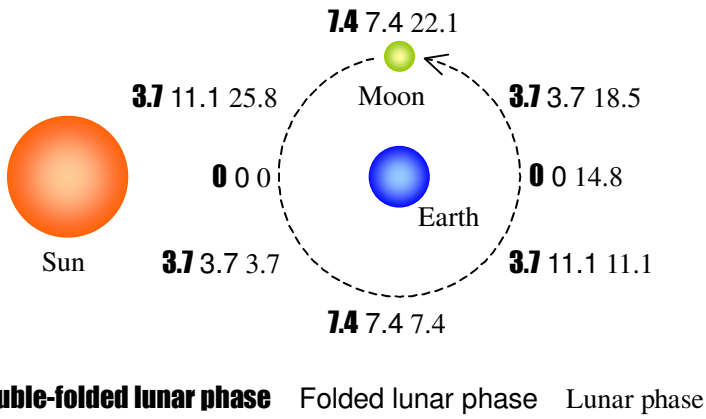

(a) Schematic figure showing (left to right) the double-folded lunar phase, folded lunar phase, and lunar phase.

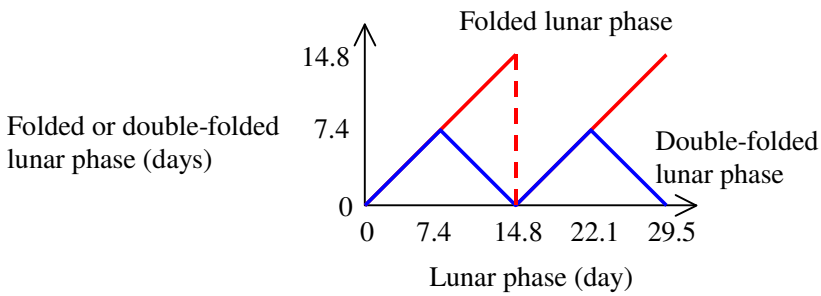

(b) Relationship between the various lunar phases

Figure 2. The lunar phase, folded lunar phase, and double-folded lunar phase.

Tanaka et al. (2002) showed a weak positive correlation between tidal stress and the occurrence of earthquakes for the approximately 12 h period by a statistical method. We previously investigated the relationships between the approximately half-month period variation and occurrences of giant earthquakes ($M_W \geq 8$) and found that giant earthquakes between 1900 and 2011 occurred at specific lunar phases at each subduction zone (Fujiii and Ozaki, 2012). In addition, occurrences of giant earthquakes tended to concentrate not only during spring tides but also during neap tides at some subduction zones. In the present study, we attempted to more clearly show the dangerous lunar phases for each subduction zone and to provide evidence to help clarify the mechanisms of giant earthquake occurrences at neap tides at some subduction zones. To this end, the concepts of folded and double-folded lunar phases were developed, and the influence of tidal stress on reverse faulting was investigated based on the strike of subduction zones.

2. Giant earthquake occurrence and lunar phase for each subduction zone

The magnitude and lunar phase of giant earthquakes from 1900–2012 are shown for each subduction zone in Figures 3a–10a. Giant earthquakes occur basically around the spring tides, but clusters also occur at other times. The clusters can be shown more clearly using a folded lunar phase (Figs. 3b–10b), which represents the 0–14.8 day period following a spring tide (Fig. 2). Clusters can be seen 1–4 days after spring tide for Peru, 3–5 days after for Indonesia, 5–7 days after for Tonga, 3–8 days after for Japan, and 8–11 days after for Kuril. On the other hand, giant earthquakes tend to be concentrated just before spring tide for Chile (0–3 days before), New Guinea (0–2 days before), and Alaska (0–2 days before). Paying sufficient attention to foreshocks and various other precursors such as GPS (Global Positioning System) anomalies (Heki, 2011) during the dangerous lunar phases for each subduction zone will be very useful for reducing damage caused by giant earthquakes.

That giant earthquakes occurred just before or at spring tides in Chile, New Guinea, and Alaska seems natural because tidal stress is largest at spring tides. However, the finding that giant earthquakes also occurred around neap tides in Peru, Indonesia, Tonga, Japan, and Kuril is unexpected.

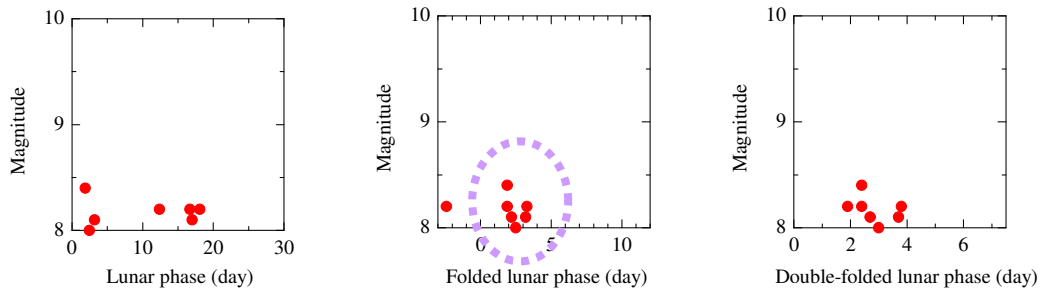

(a) (b) (c)

Figure 3. Lunar phase and giant earthquake occurrences in Peru.

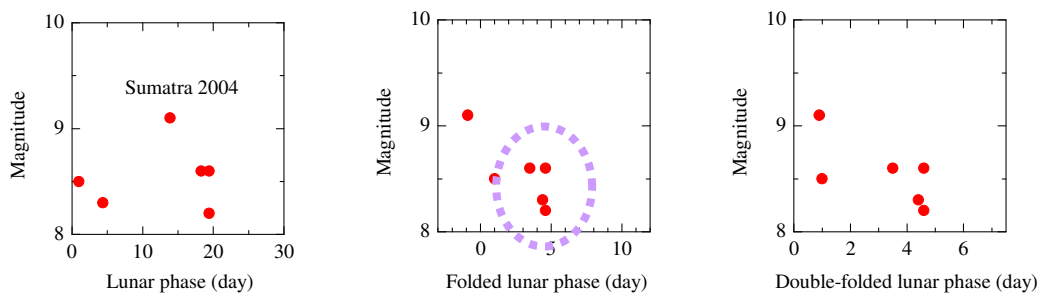

(a) (b) (c)

Figure 4. Lunar phase and giant earthquake occurrences in Indonesia.

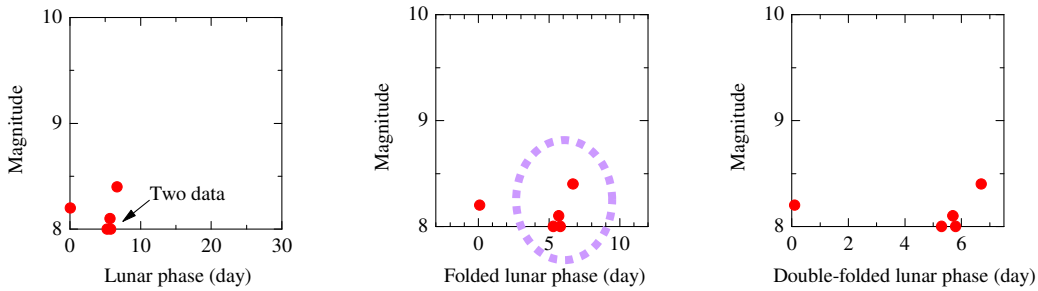

(a) (b) (c)

Figure 5. Lunar phase and giant earthquake occurrences in Tonga.

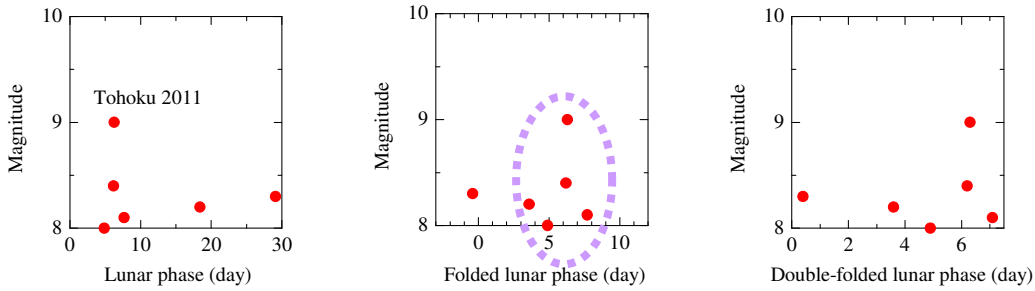

(a) (b) (c)

Figure 6. Lunar phase and giant earthquake occurrences in Japan.

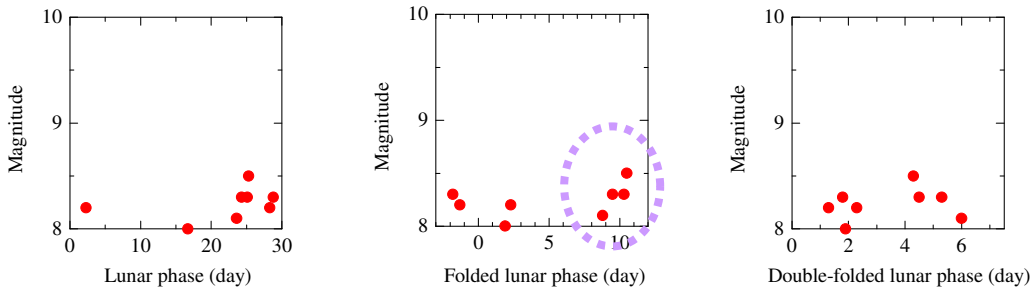

(a) (b) (c)

Figure 7. Lunar phase and giant earthquake occurrences in Kuril.

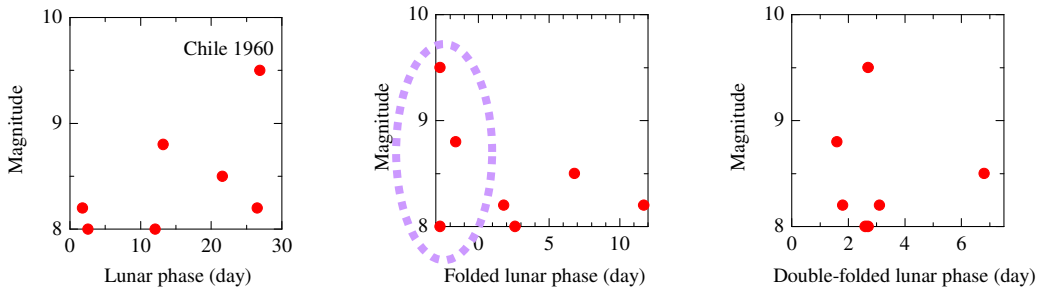

(a) (b) (c)

Figure 8. Lunar phase and giant earthquake occurrences in Chile.

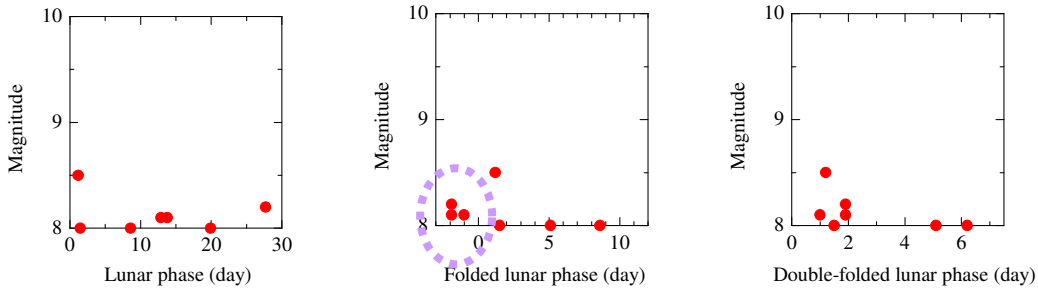

(a) (b) (c)

Figure 9. Lunar phase and giant earthquake occurrences in New Guinea.

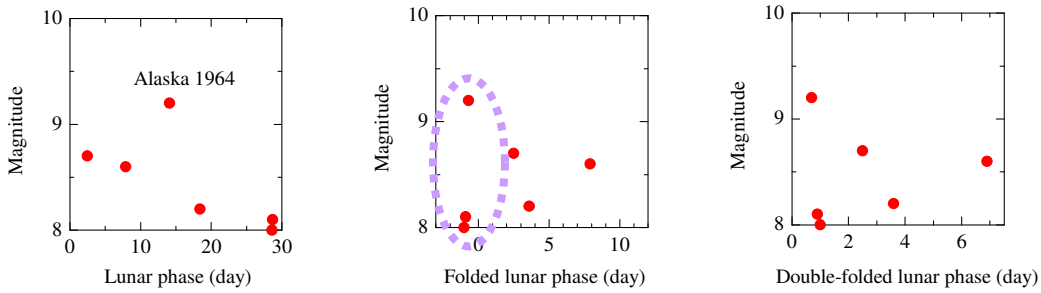

(a) (b) (c)

Figure 10. Lunar phase and giant earthquake occurrences in Alaska.

3. Mechanism of giant earthquake occurrences at neap tides

As an attempt to clarify the mechanism by which giant earthquakes can also occur at neap tide, the relationship between the strike of each subduction zone and the double-folded lunar phase (Figs. 3c–10c) of the largest earthquake at each subduction zone was examined. The double-folded lunar phase is defined as shown in Figure 2 and represents the 0–7.4 day time period separating spring tides (new or full moon) and neap tides (half moon phases). The relationship between the largest earthquake at each subduction zone and the double-folded lunar phase can be approximated by a sine curve in which the double-folded lunar phase is minimum at a strike of N66°W and maximum at a strike of N24°E with a correlation coefficient of 0.81 (Fig. 11).

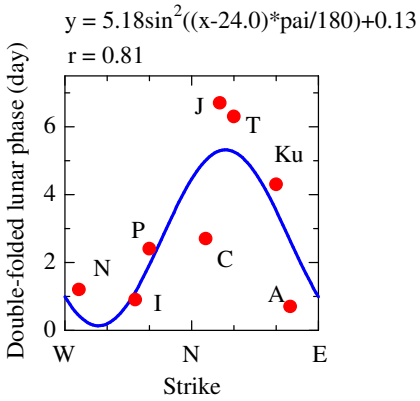

Figure 11. Representative strike and the double-folded lunar phase of the largest earthquake for each subduction zone. P: Peru, I: Indonesia, T: Tonga, J: Japan, K: Kuril, C: Chile, N: New Guinea, and A: Alaska.

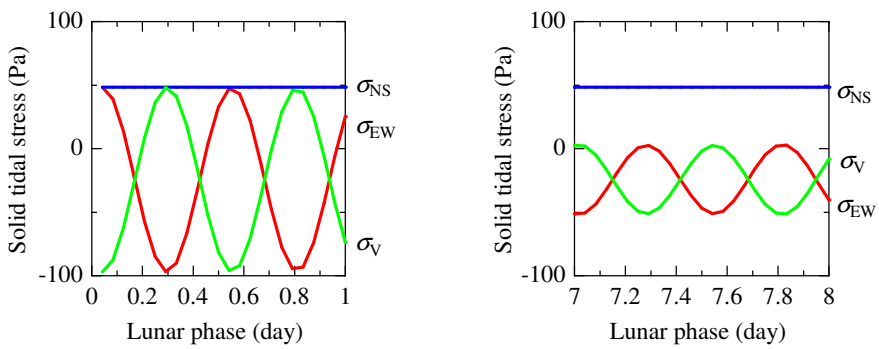

(a) Spring tide at the Equator (b) Neap tide at the Equator

Figure 12. Examples of the solid tidal stress at a depth of 10 km in the Earth with no inclination and a uniform density of 5500 kg/m^3. Compression is taken as positive.

The influence of strike on the solid tidal stress acting on a subduction zone is considered below. For simplicity, NS, instead of N24°E, and EW, instead of N66°W, subduction zones are considered and the inclination of Earth's axis of rotation is ignored. The variation in the NS component of the theoretically calculated solid tidal stress due to the lunar phase is smaller than that of the other stress components (Fig. 12). The NS stress component acts as the maximum principal stress σ_1 for reverse faulting along EW subduction zones but as the intermediate principal stress σ_2 for reverse faulting along NS subduction zones (Fig. 13). To represent the influence of the solid tidal stress on reverse faulting with a single index, the stress increment $\Delta\sigma$ is defined as follows:

$$\Delta\sigma = \Delta\sigma_1 - \alpha\Delta\sigma_2 - \frac{1+\sin\phi}{1-\sin\phi}\Delta\sigma_3 \quad (1)$$

where ϕ is the friction angle, σ_3 is the minium principal stress, and α is a constant that denotes the influence of the intermediate principal stress and seems to be ≈ 1 for small intermediate principal stress and ≈ -1 for large intermediate principal stress based on the experimental results of Takahashi and Koide (1989). A positive stress increment means that the solid tidal stress accelerates reverse faulting and *vice versa*. The amplitude and rate of the stress increment are larger at spring tide and smaller at neap tide (Fig. 14). The stress increment is smaller for EW subduction zones and even becomes 0 under some conditions (Fig. 14). Considering the fact that giant earthquakes tend to occur at neap tides at NS subduction zones, it can be inferred that the high stress increment rate prohibits the occurrence of giant earthquakes at NS subduction zones during spring tides.

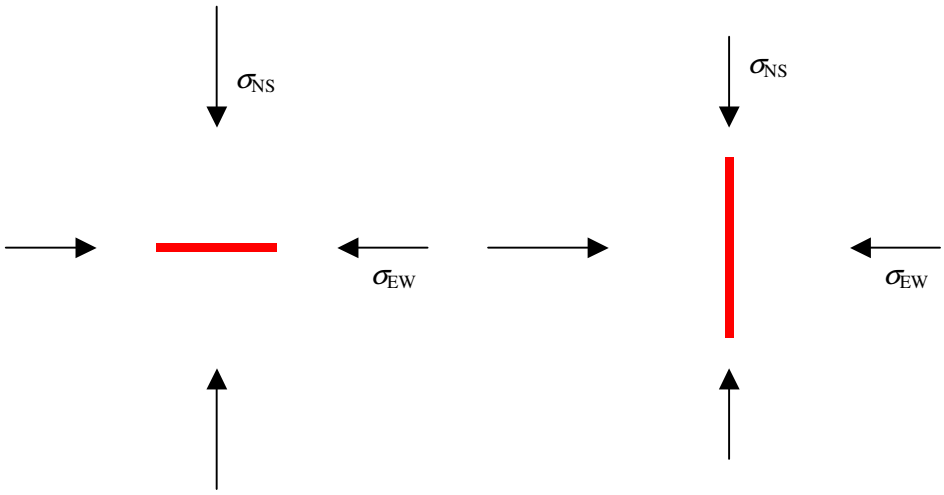

Figure 13. Schematics showing the maximum, intermediate, and minimum principal stresses for NS and EW subduction zones at the Equator.

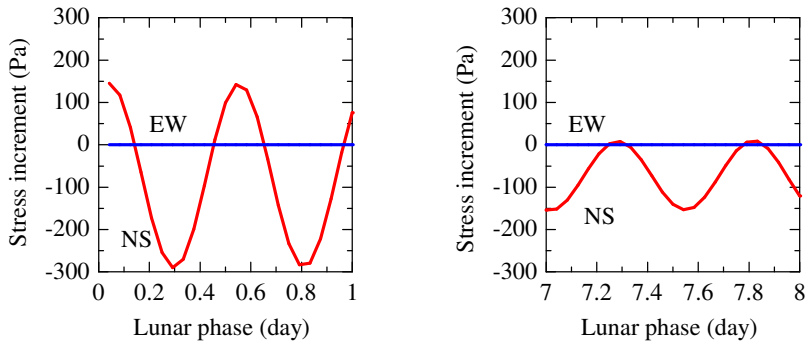

(a) Spring tide at N45° (b) Neap tide at N45°

Figure 14. Example of change in the theoretical solid tidal stress increment for NS and EW faults with $\phi = 30(^{\circ})$ and $\alpha = 1$.

The reason for this prohibition can be explained by considering the rheology of rock. Although it is not an extreme phenomenon, such as Oobleck (Zabawski, 2009), rock strength increases as the loading rate increases due to pore pressure changes accompanied by rapid dilatancy under a high loading rate, viscous deformation, and stress corrosion. The change in strength $\Delta\sigma_{\max}$ can be represented by

$$\frac{\Delta\sigma_{\max}}{\sigma^0_{\max}} = \beta \log \frac{\mathrm{d}\varepsilon / \mathrm{d}t}{(\mathrm{d}\varepsilon / \mathrm{d}t)_0} \tag{2}$$

where $\sigma^0_{\max}$ is the strength at $(\mathrm{d}\varepsilon/\mathrm{d}t)_0$, β is a constant, $\mathrm{d}\varepsilon/\mathrm{d}t$ is the strain rate, and $(\mathrm{d}\varepsilon/\mathrm{d}t)_0$ is the reference strain rate. Assuming a β of 10% and that the strain rate at spring tides is three times that at neap tides, from Figure 14, the increase in strength is calculated to be 4.8%. On the other hand, the increase in the peak value of the stress increment from neap tide to spring tide in Figure 14 is just 150 Pa, or 0.000056% of the overburden pressure at, for example, a depth of 10 km assuming a unit weight of 27 kN/m^3. The stress increment amplitude from neap tide to spring tide changes from 150 to 450 Pa, but it is still very small even considering that the tidal stress is several hundred times the solid tidal stress. The example shown in Figure 14 is an extreme case, and the questions of whether such small stress variation can cause a drastic change in strength and whether tidal stress is roughly proportional to solid tidal stress with some delay should be inspected further. However, the strength increase from neap tides to spring tides is much larger than the increase in the stress increment, and this can explain the prohibition of giant earthquakes during spring tides at NS subduction zones. The asthenosphere also exhibits viscous deformation, which might affect the occurrence of giant earthquakes. This possibility should be considered in the future.

4. Concluding remarks

The dangerous lunar phases for each subduction zone have been determined. These are, represented as the delay from spring tides, 1–4 days for Peru, 3–5 days for Indonesia, 5–7 days for Tonga, 3–8 days for Japan, 8–11 days for Kuril, -3–0 days for Chile, -2−0 days for New Guinea, and -2–0 days for Alaska. Paying sufficient attention to foreshocks and various other precursors such as GPS anomalies during the dangerous lunar phases for each subduction zone will be a very useful way to reduce damage from giant earthquakes. The reason that giant earthquakes occur not only at spring tides but also at neap tides at some subduction zones is the prohibition of giant earthquakes during spring tides that occurs by strength increases due to the rapid variation in tidal stress during spring tides at NS subduction zones.

References

Fujii, Y. and Ozaki, Y., 2012, Date, Lunar Phase and Time of Giant Earthquakes might be Specified for Each Subduction Zone, *Seismological Research Letters*, 83(2), 456 (*Seismological Society of America 2012 Annual Meeting, Apr. 19, San Diego*)

Gutzwiller, M., 1998, The Oldest Three-body Problem, *Reviews of Modern Physics*, 70(2), 589-639

Heki, K., 2011, Ionospheric Electron Enhancement Preceding the 2011 Tohoku-Oki Earthquake, *Geophys. Res. Let.*, 38, L17312, doi:10.1029/2011GL047908

Takahashi, M. and Koide, H. 1989, Effect of the Intermediate Principal Stress on Strength and Deformational Behavior of Sedimentary Rocks at the Depth Shallower than 2000 m. *Rock at Great Depth* (Rotterdam:Balkema, 1989), 1, 19–26.

Tanaka, S., Ohtake, M. and Sato, H., 2002, Evidence for Tidal Triggering of Earthquakes as Revealed from Statistical Analysis of Global Data, *J. Geophys. Res.*, 107(B10), 2211, doi:10.1029/2001JB001577

Zabawski, E., 2009, Oobleck the Dilatant, *Tribology & Lubrication Technology*, 65(10), 6